Investigation on Chemical Etching Process of FPCB With 18 μm Line Pitch

JIAZHENG SHENG[1], HUI LI[1,2], (Senior Member, IEEE), SHENGNAN SHEN[1,2], (Senior Member, IEEE), RUIJIAN MING[1], BIN SUN[3], JIAN WANG[3], DAODE ZHANG[4], AND YINGGANG TANG[4]

[1]School of Power and Mechanical Engineering, Wuhan University, Wuhan 430072, China
[2]The Institute of Technological Sciences, Wuhan University, Wuhan 430072, China
[3]Jiangsu Leader-Tech Electronics Company Ltd., Pizhou 221300, China
[4]School of Mechanical Engineering, Hubei University of Technology, Wuhan 430068, China

Corresponding authors: Hui Li (li_hui@whu.edu.cn), Bin Sun (sunbin@leader-techcn.com), and Daode Zhang (hgzdd@126.com)

ABSTRACT Flexible printed circuit boards (FPCB) are widely used in smart devices with high wiring density and light weight. In this paper, the chemical etching process of FPCB with 18 μm line pitch is investigated. A geometric model of the FPCB circuit with the shape of ''T'' is established and simulated by the finite element method. The time evolution of the etching cavity, concentration field and velocity field of $CuCl_2$ solution are studied, as well as the effects of initial concentrations and inlet velocities on the etching cavity profile. Finally, the FPCB sample with 18 μm line pitch is successfully fabricated by employing process parameters from the etching simulation. The results show that as the increase in the etching cavity, recirculating eddies form at the bottom of the photoresist in the corners of the etching cavity, resulting in more etching on the top sides of sidewalls over time. Higher initial concentration of the etching solution will result in a larger etching cavity profile, but the inlet velocity cannot affect the etching cavity profile significantly. Finally, the effectiveness of the simulation model is verified by comparing the etching cavity profiles with four experiments.

INDEX TERMS FPCB, chemical etching, transport of diluted species.

I. INTRODUCTION

With the high wiring density, light weight, thin thickness and good bendability, the flexible printed circuit board (FPCB) is widely used in full screen smartphone, smart TV with ultra-narrow bezel, flexible wearable device [1] and flexible display screen. The huge market demand promotes the progress of FPCB manufacturing process, and puts forward higher requirements on the quality of the FPCB circuit. Higher wiring density and narrower line pitch of FPCB become more and more important. Currently, the LG company in South Korea [2], Chipbond Technology Co., Ltd, Taiwan, China [3] and FLEXCEED Co., Ltd, Japan [4] have achieved the FPCB manufacturing process of 20 μm line pitch. Breaking through the manufacturing process of 18 μm or finer line pitch is crucial for the further growth of the FPCB industry.

In the production process of FPCB, there are four key manufacturing processes, namely exposure, development,

The associate editor coordinating the review of this manuscript and approving it for publication was Stavros Souravlas.

etching and tin plating. In the exposure process, it transfers the pre-designed circuit or pattern to the copper films with photoresist. Next, during the development process, the exposed photoresist is removed by a weak alkaline solution to obtain a designed circuit or pattern.

The etching process determines the quality of the formed circuit. There are some investigations on FPCB etching process. Yeh *et al.* [5] developed a modified technique of arrayed jet-stream etching to produce well-defined copper interconnects on a FPCB in a significantly shorter time, but the thickness/width of copper interconnects are 35/140 μm. Geissler *et al.* [6] devised a wet-etch chemistries that enable microcontact-printed Cu substrates to be etched with high selectivity, but this method was still far from being applied to actual production. Zhou *et al.* [7] developed a new type of nitric acid etchant with a higher etch factor value, shorter etching time, and easier waste-disposal for manufacturing fine lines.

The experimental method has a long time period and high cost. With the development of computer technology,

numerical simulation method is used to study the etching process, which reduces time and cost efficiently and can study the mechanism of the etching process. Bui *et al..* [8] studied hydrofluoric acid etching of the SiC surface using density functional theory to clarify the origin of the enhancement for the etching, which studied the etching reaction on the electronic scale. Iwakawa *et al.* [9], Ohta and Hamaguchi [10] and Hanson *et al.* [11] studied the etching process of Si based on the methods of molecular dynamics to discuss etching mechanisms on the atomic scale. van Veenendaal *et al.* [12] performed Monte Carlo simulations on silicon surface etching to explain the micromorphology of etched silicon surface and the orientation dependence of the etching rate, and Zhang *et al.* [13] described anisotropic etching of quartz using Kinetic Monte Carlo simulations to successfully predict the etching rate of a wide range of crystallographic facets, which had successfully studied the etching process on a mesoscopic scale. These methods provide good understandings of the fundamental mechanism of the etching process.

In addition, finite element method [14], [15], [18], and finite volume method [16], [17] were widely applied to model for the study in the evolution of etching process, which could study the evolution of etching boundary, flow field, concentration field and velocity field on the macro scale, and provided guidance for the production process. There are various existing numerical approaches for model calculations, including the moving-grid approach [14], [18], the variational inequality approach [19], the level-set method [20]–[22], and total concentration fixed-grid method [23], [24]. Shin and Economou [14] used a moving-grid approach to simulate convection-driven wet chemical etching, and showed that the shape evolution of etching cavities was affected by the etchant flow field, but which had not been applied to high rate anisotropic etching and verified by experiment. La Magna *et al..* [22] simulated two-dimensional profile evolution and dopant density distribution in electrochemical etching process of silicon using a level-set method for a moving front. Rath *et al..* [24] studied the wet chemical etching by proposing a total concentration fixed-grid method, which was analogous to the enthalpy method used in modeling melting/solidification processes. However, none of them studied the high-rate anisotropic of wet chemical etching, and the manufacturing process of FPCB with 18 μm line pitch or finer line pitch is still unknown.

In this paper, the chemical etching process of FPCB with 18 μm line pitch is investigated. A geometric model of the FPCB circuit is established and simulated by the finite element method. A flux equation is used to simulate a chemical reaction of the etching surface. A moving boundary condition is set to study the shape evolution of the etching cavity. The physics-controlled mesh and automatic remeshing are used to assure the simulation accuracy. The main works and contributions of this work are as follows:

1) The time evolution of the etching cavity, concentration field and velocity field of $CuCl_2$ solution is studied.

2) The effects of different initial concentrations and inlet velocities on the etching cavity profile are also examined.

3) The etching process parameters are verified by the experiment samples, and the FPCB with 18 μm line pitch is fabricated.

In *Section 2*, the description of the model formulation and method is provided. Results and discussions of simulation and experiment are shown in *Section 3*. The conclusion is drawn in *Section 4*.
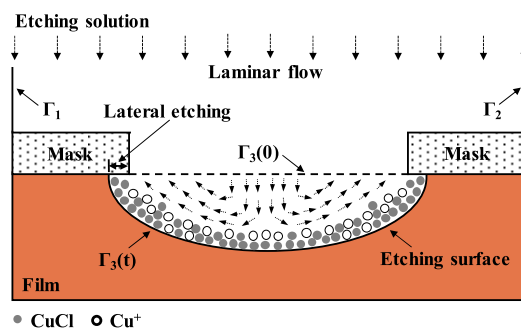

FIGURE 1. Schematic of the etching process.

II. MODEL FORMULATION AND METHOD
A. GOVERNING EQUATIONS

Fig. 1 shows the schematic of the etching process. A copper film, which partially is protected by the inert mask, is placed in an etching solution that flows through exposed film. At time zero, when $\Gamma_3(0)$ is the position of the copper film surface, it is assumed that the solution entering the etching cavity through the top contains an etchant species, which can react with the copper film but is not capable of reacting the etching mask. Through convection and diffusion, the etchant species are transported to the film surface and react thereby etching the film. As etching reaction proceeds, the time evolution of the etching cavity shape occurs according to the etching rate distribution along the cavity surface. The local fluid flow and etchant concentration distributions are affected by the deformation of the cavity, which in turn affect the further shape evolution of the cavity. $\Gamma 1$ and $\Gamma 2$ are the outlet boundaries of the flow field, and the moving etching surface $\Gamma_3(t)$ is shown at some time *t* partway during etching.

Among the etchants currently used by FPCB manufacturers, the most widely used etchant is cupric chloride ($CuCl_2$). The acidic cupric chloride has a relatively high etching rate when etching thin copper films, and the reaction products can automatically regenerate the cupric chloride, which reduces waste generation. A complex chemical reaction occurs between the $CuCl_2$ solution and exposed copper film. The net etching reaction of copper films and $CuCl_2$ solution is as follows [25]

$$Cu + CuCl_2 \rightarrow 2CuCl \qquad (1)$$

When there is an excess Cl^- in the solution, CuCl will form a complex with Cl^- and dissolve into the solution to ensure

the smooth progress of the etching reaction. As the copper films is gradually dissolved, a pre-designed circuit or pattern will be obtained on the FPCB.

In the etching simulation, through convection and diffusion, the etching solution is transported to the etching surface and react thereby etching the copper films. The etching rate of the etching surface will determine the shape of the cavity with time. The local fluid flow and etchant concentration distribution are affected the deformation of the cavity, which affects the further shape evolution of the cavity in turn. The mass flux of the etchant provided by diffusion and convection is given by equation (2) [14].

$$\frac{\partial c}{\partial t} + \mathbf{u} \cdot \nabla c = D\nabla^2 c \qquad (2)$$

where D denotes the diffusion coefficient, c is the concentration of the $CuCl_2$, and $\mathbf{u}$ is the fluid velocity of the etching solution. Combining boundary conditions and solving equation (2), the concentration distribution of the etching solution in the etching cavity can be obtained.

At the moving boundary, the flux condition is considered as in equation (3)

$$D\nabla c \cdot \mathbf{n} = -kc \qquad (3)$$

where k is the etching (surface) reaction rate constant, and $\mathbf{n}$ is the normal vector pointing outside the boundary. Equation (3) implies a first-order chemical reaction at the moving boundary [14]. The movement of the boundary is defined by

$$v = -D\nabla c \cdot \frac{M}{\rho} \cdot \mathbf{n} \qquad (4)$$

where v is the velocity of the moving boundary, M is the molar mass and ρ is the density of the copper.

B. SIMULATION MODEL

During the etching process, the FPCB will be sent to a spray etching device by a roll-to-roll transport method. The etching solution is sprayed on the surface of the FPCB through the nozzles arranged in array, and reacts with the copper films without mask protection. The 0.45 mol/L $CuCl_2$ etching solution flows into the etching cavity with the velocity of 1 m/s, and is transported by the convection and diffusion to the etching surface. The concentration distribution of $CuCl_2$ solution in the etching cavity is affected by the amount of the $CuCl_2$ etchant flux through the etching surface. The shape evolution of the etching cavity is tracked by using a moving boundary scheme.

Fig. 2 shows the geometric model of the FPCB circuit with 18 μm line pitch. It selects a local domain between the photoresist layers as the target and a simulation model with the shape of "T" is established. The distance between the neighbor photoresist layers is 8 μm. The thickness of the photoresist layer and copper layer are 2 μm and 8 μm respectively. The high-concentration $CuCl_2$ solution enters the flow field from the inlet at a certain velocity, the outlet is set on both sides, and the bottom of the model is set as a
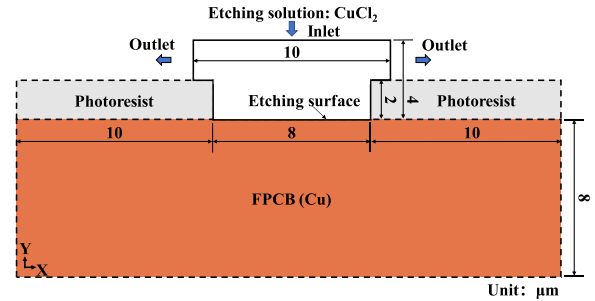
FIGURE 2. Geometric model of the FPCB circuit with 18 μm line pitch.

moving boundary (etching surface). The width of the inlet is 10 μm and the height of the outlet is 2 μm.

In this paper, the finite element method is used for analyzing the etching process with the software COMSOL (COMSOL Inc., Sweden), including the chemical species transport module for the study of the convection and diffusion of etchant, the fluid flow module for the study of the flow field of etchant, and the mathematics module for the study of the shape evolution of the etching cavity.

The following assumptions are made in the simulation:

(a) The flow of etching solution fluid is a laminar, incompressible and steady-state flow, since the size of the etching cavity is on the order of the micron.

(b) Only one etchant species in the solution is important in the etching reaction which follows linear kinetics.

(c) The etching process is anisotropic, since there is an inhibitor in the etching solution [26].

The velocity boundary condition at the inlet was set as $v_0 = 1$ m/s. At the outlet it was set as the stress boundary and the general stress was set as zero Pa. The movement of the boundary was described by equation (5) and the rest boundaries were set as stationary walls.

$$v = \alpha \cdot kc \cdot \frac{M}{\rho} \cdot \mathbf{n}_x + kc \cdot \frac{M}{\rho} \cdot \mathbf{n}_y \qquad (5)$$

where α is the anisotropic difference coefficient. $\mathbf{n}_X$ is the component of $\mathbf{n}$ in the X direction. $\mathbf{n}_Y$ is the component of $\mathbf{n}$ in the Y direction. In the concentration field of $CuCl_2$ solution, the boundary condition at the inlet was $c_0 = 0.45$ mol/L. The flux condition of etching surface was described by equation (6), and no flux conditions were set on the rest boundaries.

$$D\nabla c \cdot \mathbf{n} = -\alpha \cdot kc \cdot \mathbf{n}_x - kc \cdot \mathbf{n}_y \qquad (6)$$
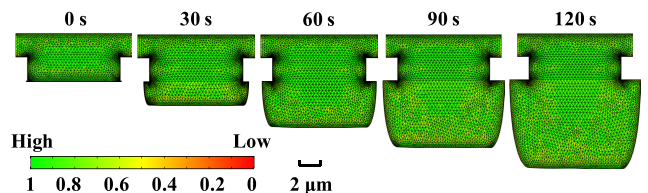
FIGURE 3. Mesh quality of free deformable mesh.

Since the etching cavity evolves with time during the etching process, the physics-controlled mesh and automatic

TABLE 1. Simulation parameters.

Items	Value
CuCl$_2$ solution concentration	0.45 mol/L*
Inlet velocity	1 m/s
Molar mass of copper	63.55 g/mol
Copper density	8960 kg/m^3
Diffusion coefficient	7.27×10^{-10} m^2/s [27]
Reaction rate constant	20.89×10^{-6} m/s*
Anisotropic difference coefficient α	0.2*

* Provided by Jiangsu Leader-Tech Electronics Co., Ltd.

remeshing are used to assure the simulation accuracy. The remeshing occurs when the mesh quality falls below a threshold value, which assures a satisfactory mesh quality throughout the simulation. As shown in Fig. 3, the mesh generated by the physics-controlled method is the triangular mesh, and the high mesh quality is achieved at different simulation stages. For example, at the end of etching process at time point of 120 s, there are 2,195 nodes and 4,208 elements generated, and the average unit mass of elements is as high as 0.93, which guarantees the accuracy of simulation results. Table 1 lists the parameters used in the simulation.

III. RESULTS AND DISCUSSIONS

In the etching chamber, the unmasked copper is etched on the surface of copper films until the copper films at the cavity bottom have been cleared. Fig. 4 shows the concentration field and velocity field of the CuCl$_2$ solution in the etched cavity at the end of the etching. The etching process costs 120 s totally. When the "etching reaction" occurs on the etching surface, the high-concentration CuCl$_2$ solution flows into the etching cavity through the inlet. It finally forms a gradient concentration distribution from the top to the bottom of the etching cavity (Fig. 4(a)). The lowest concentration of CuCl$_2$ solution appears at the bottom, which is 0.41 mol/L. With the action of diffusion, the CuCl$_2$ solution will flow from the high concentration area to the low concentration area to supplement the depletion of CuCl$_2$ solution.

Correspondingly, a laminar flow of CuCl$_2$ solution is formed in the cavity (Fig. 4(b)). In addition to the diffusion effect, along the flow direction, the high concentration solution is brought into the cavity under the action of convection. With the increase in the size of etching cavity, the etching solution flows in from the upper inlet and flows out from the outlet, which eventually forms recirculating eddies at the corners of the etching cavity, immediately beneath the photoresist. The transport effects of the main recirculating eddies are considerably more than the recirculating eddies beneath the photoresist, which fills the etching cavity. Formed eddies bring the high-concentration CuCl$_2$ solution in the cavity from the central area to the sides, which causes the CuCl$_2$ concentration on both sides to increase, as shown in Fig. 4(a), thus allowing increased lateral etching close to the bottom of the photoresist. Moreover, both distributions of
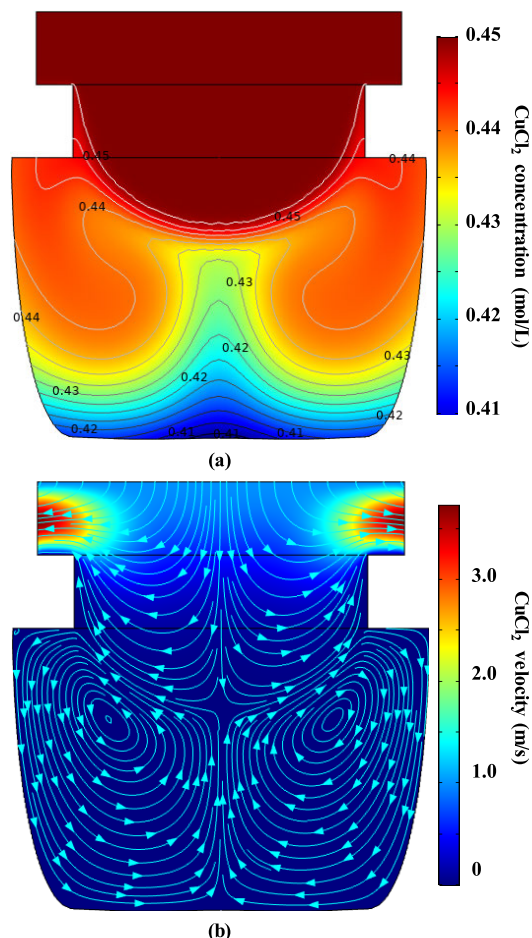

FIGURE 4. (a) Gradient concentration distribution and (b) flow field distribution of CuCl$_2$ solution in the etching cavity.

concentration and flow field are almost symmetric along the central line.
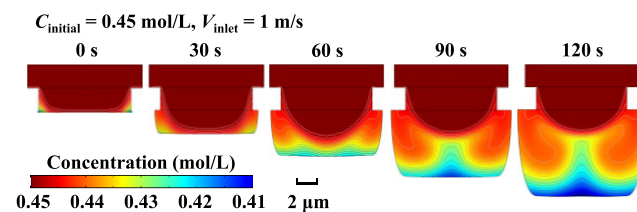

FIGURE 5. Time evolution of gradient concentration distribution of CuCl$_2$ solution in the etching cavity.

Fig. 5 shows the evolution process of the concentration distribution of CuCl$_2$ solution from the time when a FPCB enters the first etching chamber to the time when it leaves the etching line, which is at C_{initial} = 0.45 mol/L and V_{inlet} = 1 m/s. As the "etching reaction" occurs, the CuCl$_2$ solution near the etching surface is continuously consumed, and the concentration distribution of CuCl$_2$ solution changes significantly. As the cavity forms and the cavity walls become exposed to the CuCl$_2$ solution, the lateral etching of sidewalls will also occur. The bottom of the sidewalls is etched for a shorter period of time than the top, resulting in nonvertical

sidewalls. Moreover, since the etching process is anisotropic, the etching rate in the lateral direction is smaller than that in the vertical direction, the height of the cavity is much larger than its width. In addition, as the size of etching cavity increases, the eddies are gradually generated, which further affects the concentration distribution of $CuCl_2$ solution.
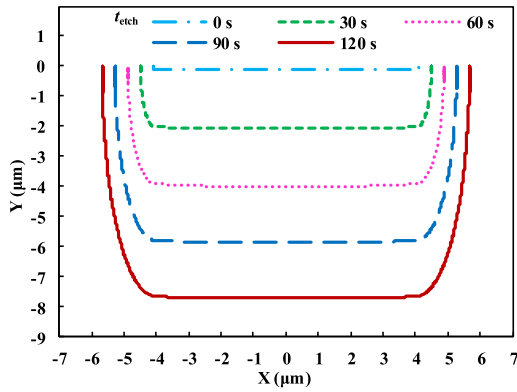

FIGURE 6. Time evolution of the etching cavity at $C_{initial} = 0.45$ mol/L and $V_{inlet} = 1$ m/s.

The cavity profiles are continuously extracted to quantitatively illustrate the evolution of the etching cavity, as shown in Fig. 6. The maximum lateral etching (defined in Fig. 1) of the sidewalls in the lateral direction is 0 μm, 0.49 μm, 0.88 μm, 1.28 μm, and 1.68 μm at different time points, respectively. The depth of the etched cavity is 0 μm, 2.06 μm, 3.98 μm, 5.85 μm, and 7.70 μm, respectively. The etch factor (EF), defined as the etched depth at the center of the cavity mouth divided by lateral etching at the bottom of the photoresist, is the indicator of the etch anisotropy achieved. In Fig. 6, the etching factor at different moments is 0, 4.20, 4.52, 4.57 and 4.58, respectively, which indicates that the etching factor gradually increases with time. The larger the etch factor, the higher the anisotropy, which indicates that the proposed method can study the anisotropy of the etching process well.

Considering the influence of $CuCl_2$ concentration on the evolution of the etching cavity, the initial concentration at the inlet boundary is investigated. Fig. 7 shows the concentration distribution of $CuCl_2$ solution in the etching cavity at different moments with different initial concentrations. It is found that the gradient concentration distribution pattern of $CuCl_2$ solution in the etching cavity does not change significantly with initial concentrations, and the evolution process of the etching cavity is roughly the same. But the size of etching cavity increases with initial concentrations.

The obtained profiles of the etching cavity at different initial concentrations are extracted as shown in Fig. 8. The maximum lateral etching of the sidewalls is 1.50 μm, 1.68 μm, 1.85 μm, and 2.02 μm, respectively. The depth of the etched cavity is 6.88 μm, 7.70 μm, 8.50 μm and 9.30 μm, respectively. In actual production, the thickness of the copper layer in the FPCB is 8 μm. When the initial concentration is 0.5 mol/L, the etching depth is greater than 8 μm and the
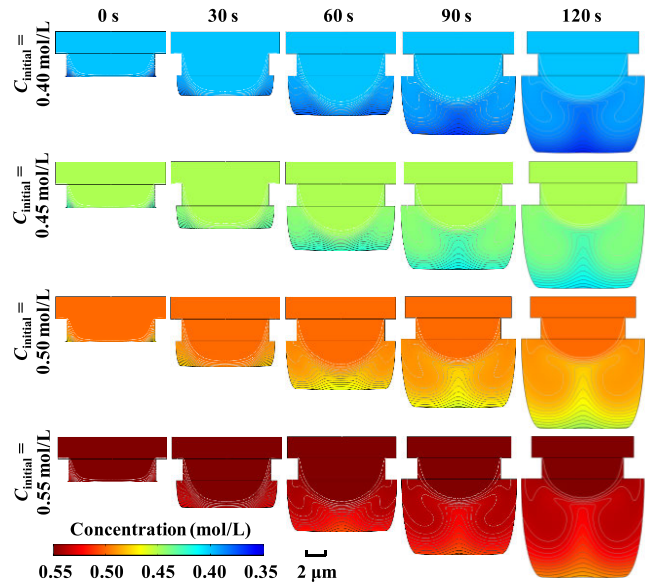

FIGURE 7. Gradient concentration distribution of $CuCl_2$ solution in the etching cavity during etching process with different initial concentrations.
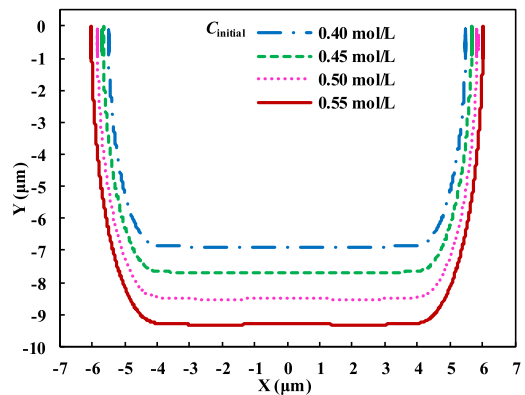

FIGURE 8. Etching surface displacement of the etching cavity at 120 s with different initial concentrations of $CuCl_2$ solution.

side etching further increase, which is not conducive to FPCB production. Therefore, the concentration of $CuCl_2$ solution during production process should be controlled at about 0.45 mol/L or less.

In the etching cavity, the distribution of the concentration field of $CuCl_2$ solution is mainly affected by the convection and diffusion, which affects the evolution of the etching cavity. Fig. 9 shows the gradient concentration distribution of $CuCl_2$ solution with different inlet velocities. With the increase of the inlet velocity, the area of the high concentration increases obviously in the etching cavity. And the maximum distribution area with high concentration occurs at the largest velocity of 7 m/s. In addition, as the inlet velocity increases, the concentration eddies in the undercut regions gradually decrease. Then the convection effects of the main recirculating eddies, which fills the cavity, gradually play a leading role.

The obtained profiles of the etching cavity at different inlet velocities are extracted as shown in Fig. 10. There is
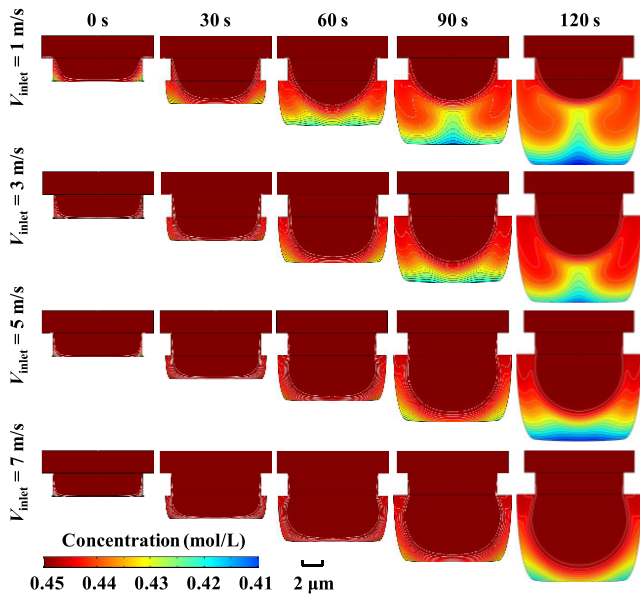
FIGURE 9. Gradient concentration distribution of CuCl$_2$ solution in the etching cavity with different inlet velocities.
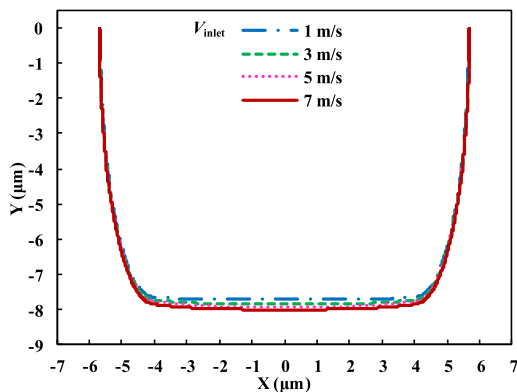

FIGURE 10. Etching surface displacement of the etching cavity at 120 s with different inlet velocities.

FIGURE 11. AFM images of four FPCB samples.
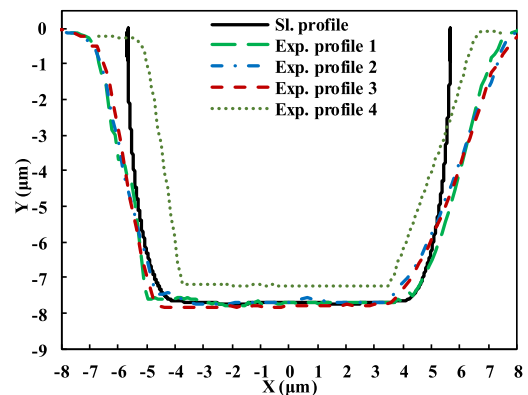
FIGURE 12. Profiles of FPCB samples obtained by simulation and experiment.

almost no difference in maximum lateral etching at the top of the sidewalls. The depth of the etched cavity is 7.70 μm, 7.82 μm, 7.89 μm, and 7.96 μm, respectively. The inlet velocity can affect the gradient concentration distribution in the etching cavity, but has little effect on the etching surface displacement of the etching cavity, because the displacement is only related to CuCl$_2$ concentration of the etching surface. There is little difference in the concentration of CuCl$_2$ solution near the etching surface at different inlet velocity. For the spray etching system, the directional projection of the sprays toward the film surface will be helpful for transport. Since the boundary layer close to the etching surface will have better penetration when the liquid velocity is enhanced.

Fig. 11 shows the three-dimensional microscopic profile of the FPCB sample by the atomic force microscope (Dimension ICON, Bruker Corporation, Billerica, MA, USA). It can be seen that the etching profiles of the samples have a good consistency, showing a "U" shape. The two-dimensional profiles of the etching cavity of four FPCB samples are further
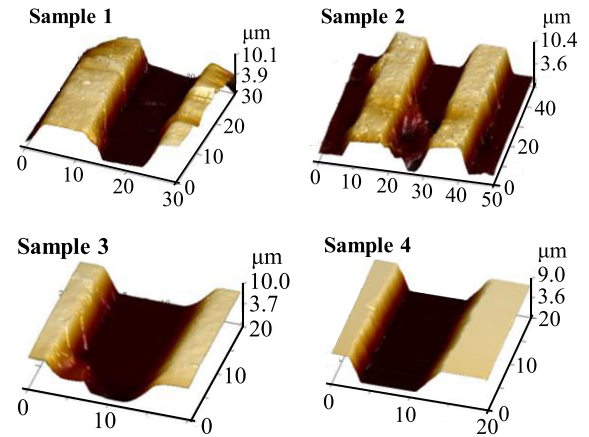
extracted and compared with the simulated profiles, as shown in Fig. 12. It can be seen that there is a good agreement, especially the etching depth in the vertical direction. It verifies that proposed method simulates the etching process of FPCB copper films well and obtained process parameters are reasonable.

Furthermore, there is no significant difference in etching profiles on the bottom sides of the sidewalls, but considerably more etching occurs on the top sides of experiment profiles. That is because that with the increase in the etching cavity, recirculating eddies form at the sidewalls of the etching cavity. The eddies have a stronger effect at the top sides than at the bottom sides of the sidewalls, which may cause more copper films at the top sides to be taken away.

IV. CONCLUSION
In this paper, it investigates the chemical etching process of FPCB with 18 μm line pitch. A geometric model of the FPCB circuit with the shape of "T" is established and simulated by the finite element method. The physics-controlled mesh and automatic remeshing are used to assure the simulation accuracy. The time evolution of the etching cavity, concentration field and velocity field of CuCl$_2$ solution are studied. Based on the obtained etching process parameters the FPCB

with 18 μm line pitch was successfully fabricated. The main results are as follows:

1) With the increase in the etching cavity, recirculating eddies form at the bottom of the photoresist in the corners of the etching cavity, which increases transport of CuCl$_2$ solution by convection.
2) The sidewalls of the etched surface are not vertical, because the top of the sidewalls is etched for a longer period of time than the bottom.
3) Higher initial concentration of the etching solution can result in a larger etching cavity profile, but the inlet velocity cannot affect the etching cavity profile significantly.
4) The concentration of CuCl$_2$ solution during production process should be controlled at about 0.45 mol/L or less.
5) More lateral etching occurs on the top sides of experiment profiles compared to the simulation profiles, which may be that more copper films on the etching surface of the top sides are taken away by recirculating eddies in the experiment.

The simulation model is proved to be effective by comparing the etching cavity profiles with the experiment sample. In next work, the manufacturing of actual FPCB by the proposed method and obtained etching process parameters will be studied, and the FPCB performance will be tested using the FPCB interconnects to further improve the etching process parameters.

REFERENCES

[1] B. Meng, W. Tang, X. Zhang, M. Han, W. Liu, and H. Zhang, "Self-powered flexible printed circuit board with integrated triboelectric generator," *Nano Energy*, vol. 2, no. 6, pp. 1101–1106, Nov. 2013.

[2] *LG Group Official Website*. Accessed: Jan. 10, 2021. [Online]. Available: http://www.lg.co.kr

[3] Chipbond Technology. *Official Website*. Accessed: Jan. 10, 2021. [Online]. Available: http://www.chipbond.com.tw/eng_index.aspx

[4] FLEXCEED. *Official Website*. Accessed: Jan. 15, 2021. [Online]. Available: http://www.flexceed.co.jp

[5] T.-K. Yeh, M.-H. Tsai, M.-Y. Wang, and C.-K. Weng, "Improved shape evolution of copper interconnects prepared by jet-stream etching," *J. Appl. Electrochem.*, vol. 38, no. 11, pp. 1495–1500, May 2008.

[6] M. Geissler, H. Schmid, B. Michel, and E. Delamarche, "Selective wet-etching of microcontact-printed Cu substrates with control over the etch profile," *Microelectron. Eng.*, vols. 67–68, pp. 326–332, Jun. 2003.

[7] G. Zhou, W. He, S. Wang, Y. Mo, K. Hu, and B. He, "Improved shape evolution of copper interconnects prepared by jet-stream etching," *IEEE Trans. Electron. Packag. Manuf.*, vol. 33, no. 1, pp. 25–30, Jan. 2010.

[8] P. Bui, A. Isohashi, H. Kizaki, Y. Sano, K. Yamauchi, Y. Morikawa, and K. Inagaki, "Study on the mechanism of platinum-assisted hydrofluoric acid etching of SiC using density functional theory calculations," *Appl. Phys. Lett.*, vol. 107, pp. 1–4, Nov. 2015, Art. no. 201601.

[9] A. Iwakawa, H. Ohta, K. Eriguchi, and K. Ono, "Numerical investigation on origin of microscopic surface roughness during Si etching by chemically reactive plasmas," *Jpn. J. Appl. Phys.*, vol. 47, no. 8, pp. 6464–6466, Aug. 2008.

[10] H. Ohta and S. Hamaguchi, "Molecular dynamics simulation of silicon and silicon dioxide etching by energetic halogen beams," *J. Vac. Sci. Technol. A, Vac., Surf., Films*, vol. 19, no. 5, pp. 2373–2381, Sep. 2001.

[11] D. E. Hanson, A. F. Voter, and J. D. Kress, "Molecular dynamics simulation of reactive ion etching of Si by energetic CI ions," *J. Appl. Phys.*, vol. 82, no. 7, pp. 3352–3559, Oct. 1997.

[12] E. van Veenendaal, J. van Suchtelen, P. van Beurden, H. M. Cuppeo, W. J. P. van Enckevort, A. J. Nijdam, M. Elwenspoek, and E. Vlieg, "Monte Carlo simulation of wet chemical etching of silicon," *Sensors Mater.*, vol. 13, no. 6, pp. 343–350, Dec. 2001.

[13] H. Zhang, Y. Xing, Y. Li, M. A. Gosálvez, and X. Qiu, "Kinetic Monte Carlo method for the simulation of anisotropic wet etching of quartz," *Sens. Actuators A, Phys.*, vol. 256, pp. 24–34, Apr. 2017.

[14] C. B. Shin and D. J. Economou, "Effect of transport and reaction on the shape evolution of cavities during wet chemical etching," *J. Electrochem. Soc.*, vol. 136, no. 7, pp. 1997–2004, Jul. 1989.

[15] J. A. Giddings, Y. M. Stokes, K. J. Bachus, and H. Ebendorff-Heidepriem, "Wet chemical etching of single-bore microstructured silicon dioxide fibers," *Phys. Fluids*, vol. 32, no. 7, Jul. 2020, Art. no. 073314.

[16] P. Rath and J. C. Chai, "Modeling convection-driven diffusion-controlled wet chemical etching using a total-concentration fixed-grid method," *Numer. Heat Transf., B, Fundam.*, vol. 53, no. 2, pp. 143–159, Dec. 2007.

[17] R. Ming, H. Li, S. Shen, J. Sheng, J. Wang, and B. Sun, "Investigation on etching process of FPCB with 18 μm line pitch," Jan. 2021.

[18] C. B. Shin and D. J. Economou, "Forced and natural convection effects on the shape evolution of cavities during wet chemical etching," *J. Electrochem. Soc.*, vol. 138, no. 2, pp. 527–538, Feb. 1991.

[19] C. Vuik and C. Cuvelier, "Numerical solution of an etching problem," *J. Comput. Phys.*, vol. 59, no. 2, pp. 247–263, Jun. 1985.

[20] A. Toifl, M. Quell, X. Klemenschits, P. Manstetten, A. Hössinger, S. Selberherr, and J. Weinbub, "The level-set method for multi-material wet etching and non-planar selective epitaxy," *IEEE Access*, vol. 8, pp. 115406–115422, Jul. 2020.

[21] D. Adalsteinsson and J. A. Sethian, "A level set approach to a unified model for etching, deposition, and lithography I: Algorithms and two-dimensional simulations," *J. Comput. Phys.*, vol. 120, no. 1, pp. 128–144, Aug. 1995.

[22] A. La Magna, G. D'Arrigo, G. Garozzo, and C. Spinella, "Computational analysis of etched profile evolution for the derivation of 2D dopant density maps in silicon," *Mater. Sci. Eng., B*, vol. 102, nos. 1–3, pp. 43–48, Sep. 2003.

[23] Y. C. Lam, J. C. Chai, P. Rath, H. Zheng, and V. M. Murukeshan, "A fixed-grid method for chemical etching," *Int. Commun. Heat Mass Transf.*, vol. 31, no. 8, pp. 1123–1131, Nov. 2004.

[24] P. Rath, J. C. Chai, Y. C. Lam, V. M. Murukeshan, and H. Zheng, "A total concentration fixed-grid method for two-dimensional wet chemical etching," *J. Heat Transf.*, vol. 129, no. 4, pp. 509–516, Apr. 2007.

[25] A. S. Kao, H. G. Stenger, C. Georgakis, K. L. Covert, and J. A. Kurowski, "Etch profile development in spray etching processes," *J. Electrochem. Soc.*, vol. 139, no. 8, pp. 2202–2211, Aug. 1992.

[26] Leader-Tech Electronics. *Official Website*. Accessed: Jan. 15, 2021. [Online]. Available: http://www.leader-techcn.com

[27] Z. Wu, "Determination of diffusion coefficient of CuCl$_2$ in aqueous solution," *Acta Metallurgica Sinica, English Lett.*, vol. 5, no. 1, pp. 21–27, Feb. 1992.

JIAZHENG SHENG was born in Xinyang. He received the B.E. degree from the Henan University of Technology, Zhengzhou, in 2016, and the M.E. degree in mechanical engineering from Xiamen University, Xiamen, in 2019. He is currently pursuing the Ph.D. degree with Wuhan University.

His research interest includes the optimization of FPCB processing technology.

HUI LI (Senior Member, IEEE) received the B.E. degree from the Huazhong University of Science and Technology, Wuhan, China, in 1999, and the Ph.D. degree in electrical and computer engineering from the National University of Singapore, Singapore, in 2007.

He is currently a Professor with Wuhan University, China. His research interests include design of micro/nanoelectromechanical systems and reliability of electronic product.

SHENGNAN SHEN (Senior Member, IEEE) received the B.E. degree from the Harbin Institute of Technology, Weihai, China, in 2005, and the Ph.D. degree in mechanical and aerospace engineering from Nanyang Technological University, Singapore, in 2013.

She is currently an Associate Professor with Wuhan University, China. Her research interests include precision mechanical design and design and application of high-precision positioning control.

JIAN WANG was born in Cangzhou. He received the B.E. degree from the Hebei University of Technology, Tianjin, in 2007.

He is currently a Development Manager with Jiangsu Leader-Tech Electronics Company Ltd. His research interests include the development of multi-layer blind hole FPCB technology and high-precision FPCB technology.
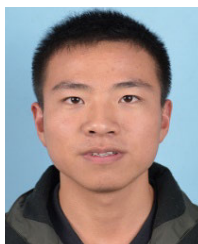
RUIJIAN MING was born in Shiyan. He received the B.E. degree from the China University of Geosciences, Wuhan, in 2020. He is currently pursuing the master's degree with Wuhan University.

His research interest includes the FPCB processing technology.

DAODE ZHANG received the B.E. degree from the Hubei University of Technology, Wuhan, China, in 1995, and the Ph.D. degree from the Huazhong University of Science and Technology, in 2009.

He is currently a Professor with the Hubei University of Technology. His research interests include the intelligent control of electromechanical equipment and machine vision.

BIN SUN was born in Qingzhou. He received the B.E. degree from the Zhongnan University of Economics and Law, Wuhan, in 2003.

He is currently a Deputy General Manager with Jiangsu Leader-Tech Electronics Company Ltd. His research interests include the production line development and industrialization of FPCB.

YINGGANG TANG was born in Liling. He received the B.E. degree from Hunan Applied Technology University, Changde, in 2020. He is currently pursuing the master's degree with the Hubei University of Technology.

His research interest includes the experimental research of FPCB processing technology.

• • •